ESI to accompany

What a difference a tail makes: 2D→2D parallel interpenetration of sheets to interpenetrated nbo networks using ditopic-4,2':6',4''-terpyridine ligands

Y. Maximilian Klein,[a] Alessandro Prescimone,[a] Markus Neuburger,[a] Edwin C. Constable[a] and Catherine E. Housecroft*[a]

Table 1 Effects of lengthening of the alkoxy tail on unit cell parameters of related compounds.

Compound	Alkyl substituent	Space group	*a* / Å	*b* / Å	*c* / Å	*β* / deg	Reference
$[\{Zn_2Cl_4(\mathbf{4})\}]_n$	^{n}hexyl	*C*2/*c*	20.4985(9)	11.6491(3)	23.7457(10)	91.737(4)	This work
$[\{Zn_2Cl_4(\mathbf{2})\}\cdot 4H_2O]_n$	^{n}octyl	*C*2/*c*	20.6102(6)	11.5999(6)	23.8198(12)	90.978(3)	[a]
$[\{Zn_2Br_4(\mathbf{2})\}]_n$	^{n}octyl	*C*2/*c*	20.6639(16)	11.9145(10)	23.6388(17)	92.289(5)	[b]
$[Zn_2Cl_4(\mathbf{5})\cdot 2MeOH]_n$	^{n}decyl	*C*2/*c*	20.777(2)	11.6382(9)	23.8738(17)	90.074(7)	This work

[a] E.C. Constable, C.E. Housecroft, S. Vujovic and J.A. Zampese, *CrystEngComm,* 2014, **16**, 3494; E.C. Constable, C.E. Housecroft, S. Vujovic and J.A. Zampese, *CrystEngComm,* 2017, DOI: 10.1039/c7ce90062g.

[b] S. Vujovic, E.C. Constable, C.E. Housecroft, C.D. Morris, M. Neuburger and A. Prescimone, *Polyhedron*, 2015, **92**, 77.

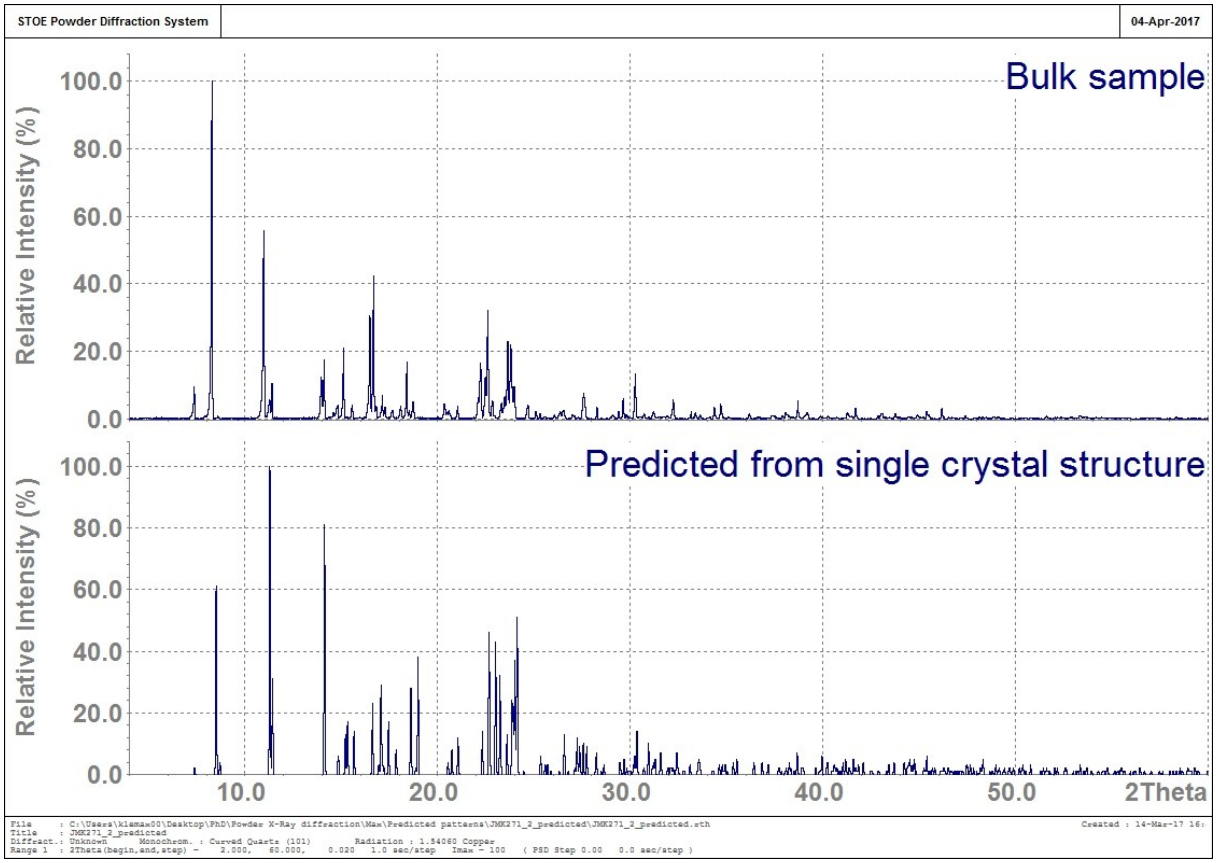

Fig. S1. X-ray powder diffraction patterns of the bulk sample of $[Zn_2Cl_4(\mathbf{5})\cdot 2MeOH]_n$ (≈295 K) compared to the predicted pattern from the single crystal data (123 K).

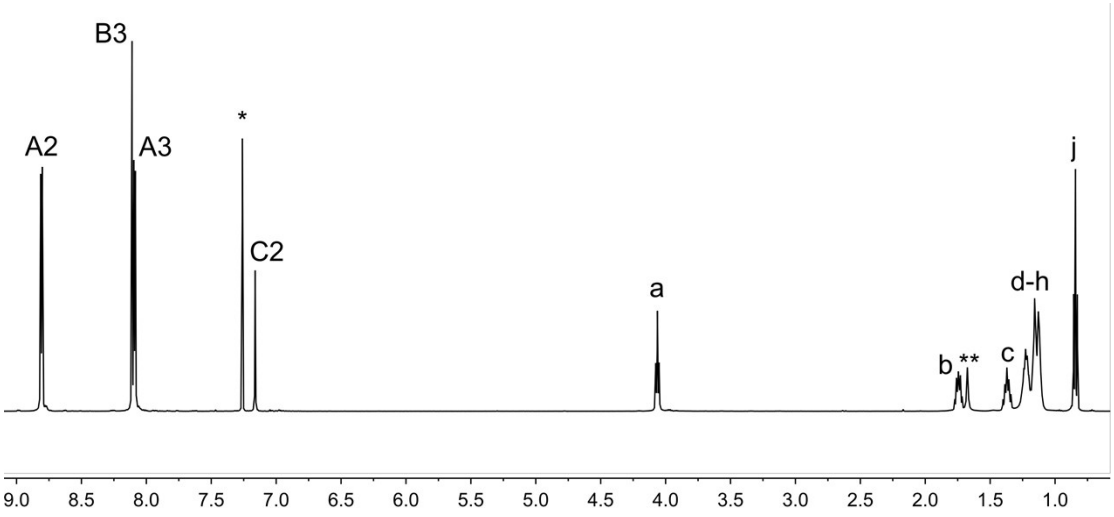

Fig. S2. The 500 MHz ^{1}H NMR spectrum of a $CDCl_3$ solution of compound **5**. * = residual $CHCl_3$; ** = water.

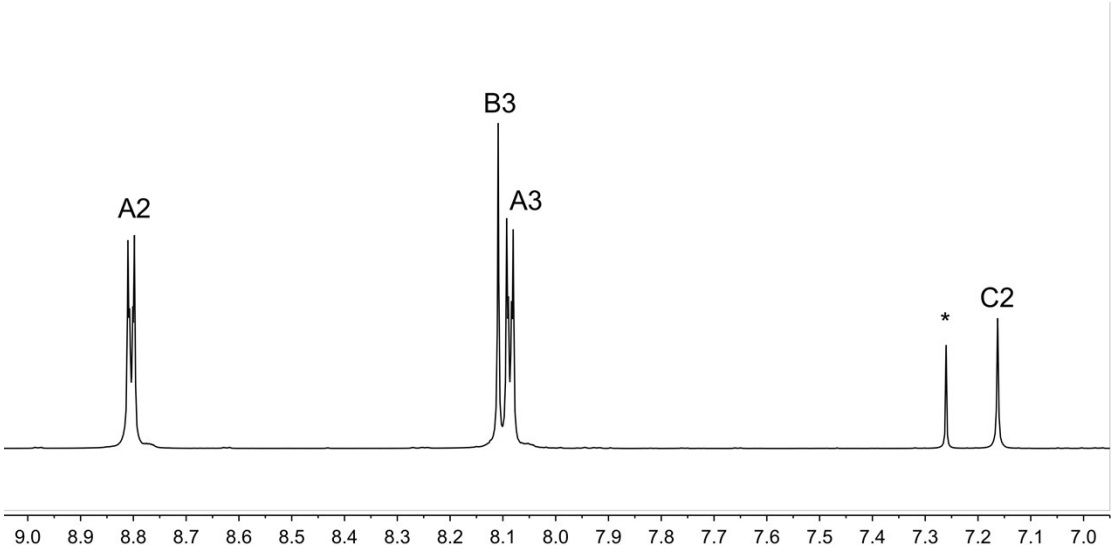

Fig. S3. The aromatic region of the 500 MHz ^{1}H NMR spectrum of a $CDCl_3$ solution of compound **4**. * = residual $CHCl_3$.

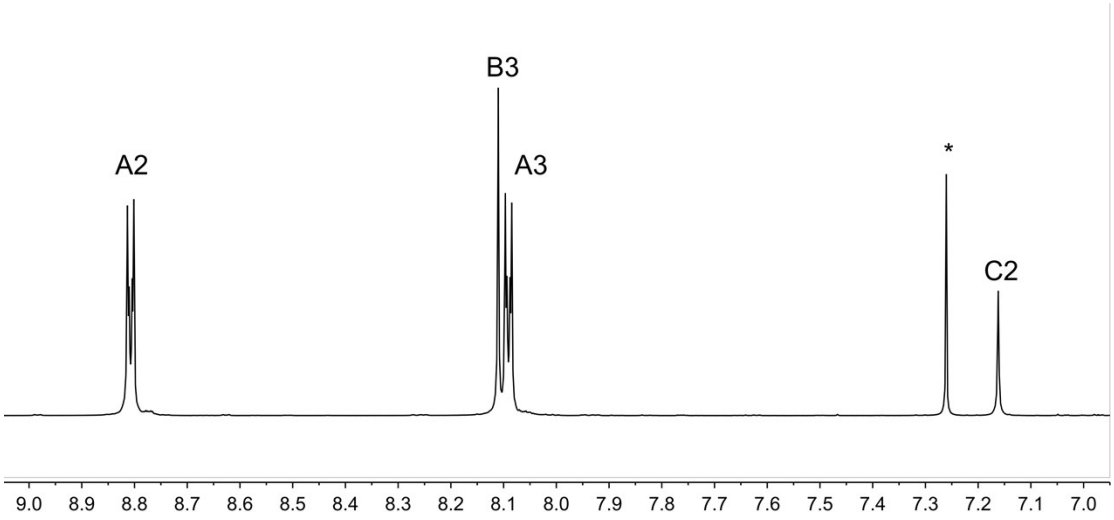

Fig. S4. The aromatic region of the 500 MHz ^{1}H NMR spectrum of a $CDCl_3$ solution of compound **5**. * = residual $CHCl_3$.

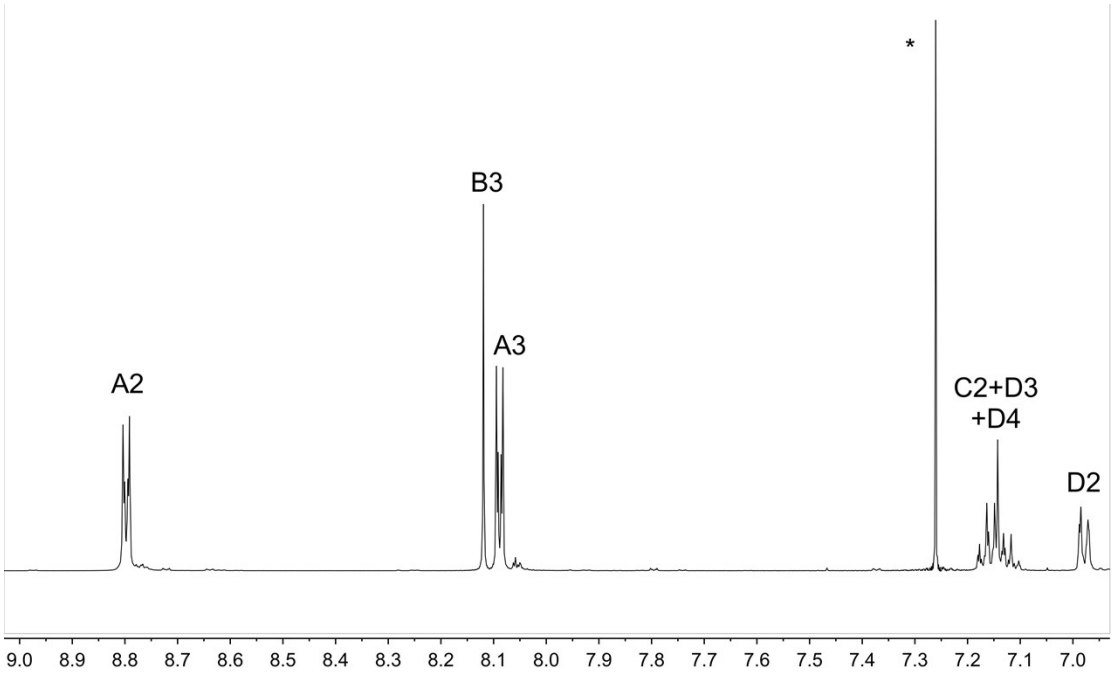

Fig. S5. The aromatic region of the 500 MHz ^{1}H NMR spectrum of a $CDCl_3$ solution of compound **6**. * = residual $CHCl_3$.

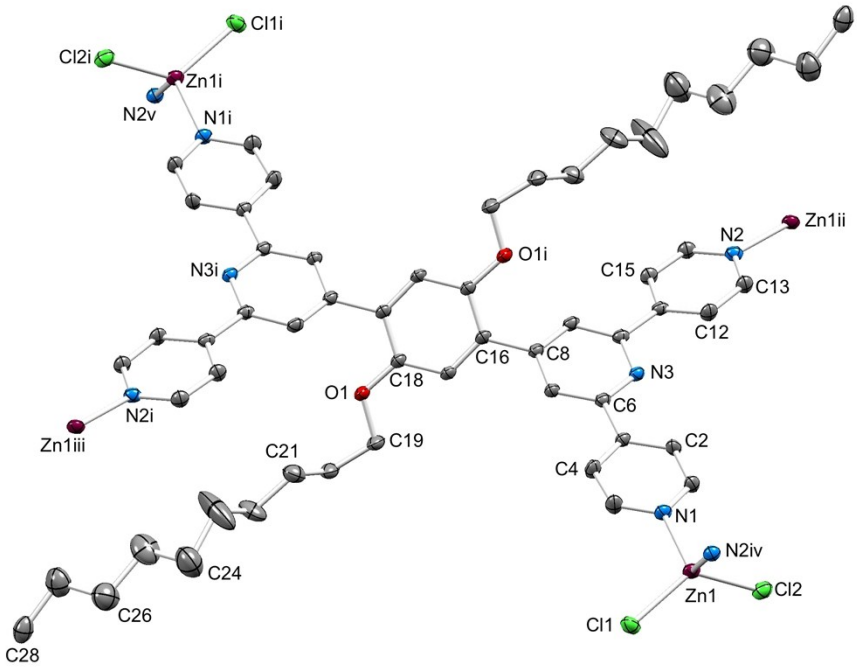

Fig. S6. The repeat unit (with symmetry generated atoms) in $[Zn_2Cl_4(\mathbf{5})\cdot 2MeOH]_n$. (H atoms omitted; ellipsoids plotted at 30% probability level). Symmetry codes: i = 1–*x*, 2–*y*, 1–*z*; ii = *x*, 1–*y*, $^1/_2$+*z*; iii = 1–*x*, 1+*y*, $^1/_2$–*z;* iv = *x*, 1–*y*, –$^1/_2$+*z;* v = 1–*x*, 1+*y*, $^3/_2$–*z*. Selected bond parameters: Zn1–N2^{iv} = 2.031(3), Zn1–Cl1 = 2.2185(12), Zn1–Cl2 = 2.2294(12), Zn1–N1 = 2.033(3), C18–O1–1.365(5), C19–O1–1.435(5) Å; N2^{iv}–Zn1–Cl1 = 104.65(10), N2^{iv}–Zn1–Cl2 = 104.44(10), Cl1–Zn1–Cl2 = 122.26(5), N2^{iv}–Zn1–N1 = 112.67(13), Cl1–Zn1–N1 = 106.80(10), Cl2–Zn1–N1 = 106.18(10), C19–O1–C18 = 118.6(3)°.

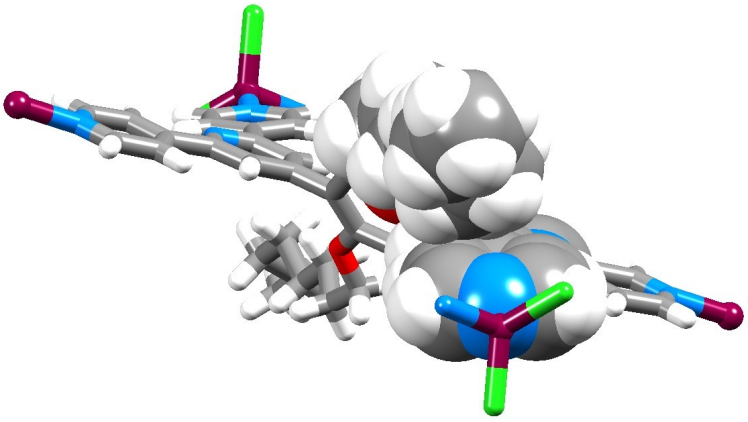

Fig. S7. Orientation of an ^{n}octyl chain over a 4,2':6',4''-tpy domain in $[\{Zn_2Cl_4(\mathbf{2})\}\cdot 4H_2O]_n$ (CSD refcode NOTPUJ).

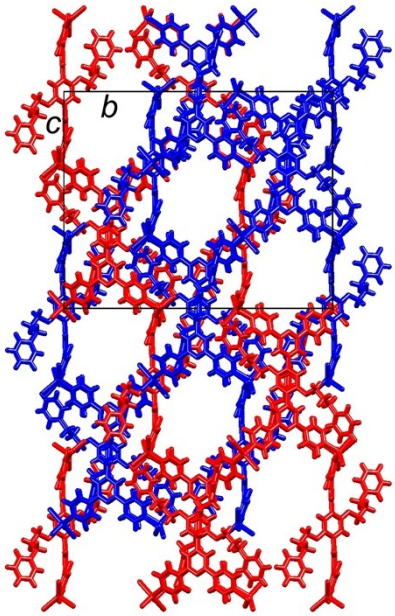

Fig. S8. Parts of interpenetrated nets (red and blue) in $[Zn_2Br_4(\mathbf{6})\cdot H_2O]_n$ view ed down the *a*-axis.